

Thermal stability of low-oxygen SiC fibers fired under different conditions

TOSHIO SHIMOO, KIYOHITO OKAMURA

*Department of Metallurgy and Materials Science, College of Engineering,
Osaka Prefecture University, 1-1, Gakuen-cho, Sakai-shi,
Osaka-fu 59-8531, Japan*

I. TSUKADA

*Graduate Student, Osaka Prefecture University, 1-1, Gakuen-cho, Sakai-shi,
Osaka-fu 599-8531, Japan*

T. SEGUCHI

*Takasaki Radiation Chemistry Research Establishment, Japan Atomic Energy Research
Institute, 1233, Watanuki-machi, Takasaki-shi, Gunma-ken 370-12, Japan*

To fabricate the low-oxygen SiC fibers with excellent thermal stability, electron-beam irradiation polycarbosilane fibers were fired for holding time of 3.6, 18 and 36 ks at each temperature of 1273 to 1573 K, and subsequently the high-temperature exposure test was carried out at 1873 K. As-fired fibers and exposed fibers were characterized by thermogravimetry, chemical analysis, Auger electron spectroscopy, resistivity measurement and tensile test. The strength of both as-fired fibers and fibers exposed to 1873 K increased with prolonging the holding time of firing treatment below 1473 K. On the contrary, a long time firing treatment at 1573 K was no longer effective for the strengthening of the low-oxygen SiC fiber. © 1999 Kluwer Academic Publishers

1. Introduction

At the present time, polycarbosilane (PCS)-derived SiC fibers are frequently used as reinforcing materials in the fabrication of ceramic matrix composites. SiC fibers have the microstructure which is composed of β -SiC crystallites, free carbon and amorphous oxycarbide, SiC_xO_y . The SiC_xO_y phase which is unstable at high temperature decomposes to β -SiC crystals by evolving SiO and CO, causing loss of fiber strength [1–12]. Therefore, high-oxygen SiC fiber fabricated by oxidation-curing method, i.e., Nicalon deteriorates severely at 1573 K and above, because of high content of SiC_xO_y phase. Thus, the electron-beam irradiation curing method has been developed for reduction of oxygen, that is, SiC_xO_y in fibers [13, 14]. Low-oxygen SiC fiber fabricated by this method, Hi-Nicalon, retained a considerable level of tensile strength even after 3.6 ks of exposure at 1973 K, though Nicalon lost the strength after exposure at 1873 K [15, 16].

SiC fibers are manufactured by firing cured PCS fibers at temperatures from 1273 to 1573 K. During firing treatment, PCS fibers liberate hydrogen as CH_4 and H_2 gas to be converted into inorganic SiC fibers. We investigated the conversion mechanism from the electron beam irradiation-cured (EB-cured) PCS fiber to low-oxygen SiC fiber by analyzing the gases evolved during heat treatment [17, 18]. As a result, it was found that the evolution of CH_4 and H_2 gas by the breakage of Si–H and Si– CH_3 bonds in PCS chain was

completed at about 1000 K and H_2 evolution by the breakage of C–H bonds was allowed to continue in the temperature range of 1000–1800 K. Therefore, a short period firing at low temperatures would incompletely result in the transition of organic PCS fiber to inorganic SiC fiber, i.e., ceramization. Imperfect ceramization is considered to have a deleterious effect on the high-temperature properties of SiC fibers. The establishment of the most appropriate firing condition of the electron beam irradiation-cured (EB-cured) PCS fiber is required in order to develop the strength of low-oxygen SiC fiber at elevated temperature.

The pyrolysis process from EB-cured PCS fiber has been investigated and the comparison of low-oxygen SiC fiber with commercial Si–C–O fiber (Nicalon) has been carried out by Chollon *et al.* [19]. However, the effects of firing conditions on the properties of low-oxygen SiC fiber have not yet been studied in detail. In previous report, low oxygen SiC fiber prepared from EB-cured fibers by firing at different heating rate from 50 to 300 $\text{K} \cdot \text{h}^{-1}$ [20]. Consequently, it was found that the fiber fired at slow heating rate exhibits an excellent thermal stability. Both the final temperature and holding time at firing treatment also should be considered as the controlling factors for the thermal stability improvement of SiC fiber. In present work, therefore, EB-cured PCS fibers were fired to various types of SiC fiber by changing the holding time from 3.6 to 36 h at temperatures between 1273 and 1573 K, and then the

fired fibers were exposed to further high temperature. The chemical, microstructural, electrical and mechanical properties of as-fired and exposed fibers were investigated, and the optimum firing condition of EB-cured PCS fibers was discussed.

2. Experimental

The specimen employed in this study was the electron-beam irradiation cured polycarbosilane (EB-cured PCS) fiber supplied by Nippon Carbon Co. Its chemical composition is shown in Table I. EB-cured fiber is characterized by a slight amount of oxygen and a large excess of carbon relative to stoichiometric SiC.

The firing treatment of EB-cured PCS fibers was carried out as follows: 4 g fibers of 100 mm in length were placed on a silica boat and then were positioned in the hot zone of a horizontal SiC resistance furnace fitted with an alumina reaction tube of 50 mm in inner diameter. After evacuation, argon was allowed to flow into the reaction tube at flow rate of $1.67 \times 10^{-6} \text{ m}^3 \cdot \text{s}^{-1}$. The fibers were continuously heated at $300 \text{ K} \cdot \text{h}^{-1}$, and were held for 3.6, 18 or 36 ks at each temperature of 1273, 1373, 1473 and 1573 K. Then, they were cooled in the furnace to the room temperature at $200 \text{ K} \cdot \text{h}^{-1}$.

High-temperature exposure test of as-fired fiber was conducted with a carbon resistance furnace equipped with a thermobalance. One gram fiber of 3 cm length was charged in a graphite crucible and then was isothermally heated for 3.6 ks in the hot zone of the furnace held at 1873 K. Argon gas was flowed from the bottom of the furnace at flow rate of $2.5 \times 10^{-5} \text{ m}^3 \cdot \text{s}^{-1}$. The mass change was recorded automatically during each run. Upon completion of TG measurement, the fiber was cooled rapidly by raising the crucible to the low temperature zone of the furnace.

The bulk composition of fibers was determined by chemical analysis: gravimetric method for the determination of Si and combustion method for the determination of C, O and H. In addition, the surface composition was determined by Auger electron spectroscopy (AES). Then, the microstructure of fibers was examined with the X-ray diffractometer and the scanning electron microscope (Hitachi Ltd., Type S5400). Using the two-terminal method, the specific resistivity was determined by applying direct current. Both ends of a monofilament were attached with electroconductive resin (Fujikura Kasei Co., Dotite) to the copper electrode plates which were 0.8 mm apart in distance. The values of resistivity were the average of 10 measurements. Furthermore, the tensile strength of a monofilament of 10 mm gauge length was determined with a tensilon-type machine (Orientec Co., Type UTM-II-20) and a load cell of 100 g at a crosshead speed of $2 \text{ mm} \cdot \text{min}^{-1}$. The mean value of 20 measurements was taken for each fiber.

3. Results

3.1. Gas evolution and bulk composition

During firing treatment, EB-cured PCS fiber generates H_2 and CH_4 gas, resulting in the mass loss. The amounts of gas evolved were determined by the difference between the mass of the fiber before and after firing. The

TABLE I Chemical composition of fibers fired under different conditions

Fiber	Si (at%)	C (at%)	O (at%)	H (at%)	C/Si ratio
As-received fiber (EB-cured PCS fiber)	15.0	27.5	0.5	56.9	1.83
As-fired fiber					
A (1273 K, 3.6 ks)	33.1	53.6	1.6	11.7	1.62
B (1273 K, 36 ks)	36.0	57.5	1.6	4.8	1.60
C (1573 K, 3.6 ks)	36.8	61.1	1.6	0.5	1.66
D (1573 K, 36 ks)	37.6	60.6	1.3	0.5	1.61

*Silicon: error of $\pm 0.5\%$ (gravimetric method).

**Carbon, oxygen, hydrogen: error of $\pm 5\%$ (combustion method).

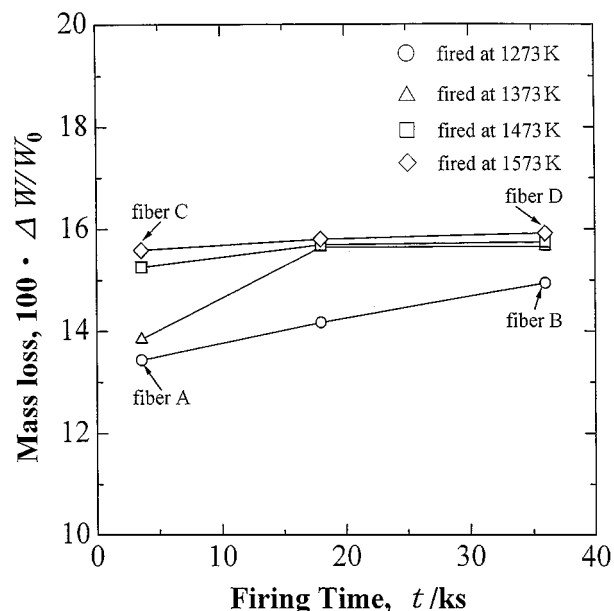


Figure 1 Mass loss of EB-cured PCS fibers during firing treatment.

observed values of mass loss are shown in Fig. 1. W_0 and ΔW are the initial mass of EB-cured PCS fiber and the mass loss occurred during firing, respectively. The mass loss increased by long period firing at higher temperature. The firing treatment occurs an organic-inorganic transition, i.e., ceramization, accompanying the generation of H_2 and CH_4 gases. When $100 \cdot \Delta W / W_0 \approx 16$, the ceramization of fiber appears to be nearly complete.

Table I shows the analytical values of EB-cured PCS fiber and fibers fired under different conditions. The cured PCS fiber with low oxygen content was fabricated by adopting EB-curing method. However, as well as oxidation-cured PCS fiber, it contained large amounts of hydrogen and an excess of carbon relative to stoichiometric SiC. It is natural that the firing treatment causes a decrease in hydrogen content. However, substantial amounts of hydrogen were retained in the fiber fired at low temperature and for short periods. The reduction of C/Si ratio implies that not only H_2 but also CH_4 gas evolved during firing treatment. It is noted that the oxygen content in the fiber fired for 36 ks at 1573 K was lower than that in other fibers. From the fact that C/Si ratio was reduced by prolonging the firing time, the low oxygen content is attributable to the evolution of CO gas.

TG curves and chemical composition of the fibers exposed to 1873 K are shown in Fig. 2 and Table II,

TABLE II Chemical composition of fibers exposed for 3.6 ks at 1873 K

Fiber	Si (at%)	C (at%)	O (at%)	H (at%)	C/Si ratio
A (1273 K, 3.6 ks)	38.5	60.1	1.5	trace	1.56
B (1273 K, 36 ks)	38.1	60.4	1.5	trace	1.59
C (1573 K, 3.6 ks)	37.5	61.4	1.1	trace	1.64
D (1573 K, 36 ks)	37.9	61.0	1.1	trace	1.61

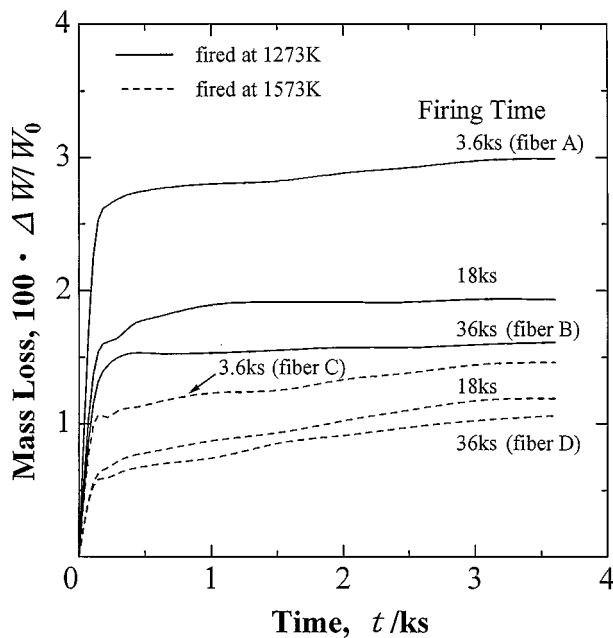


Figure 2 TG curves of as-fired fibers during 3.6 ks of exposure to 1873 K.

respectively. The mass loss occurred abruptly within 300 s of exposure and then was allowed to continue slowly. From comparison of Table I with Table II, it is clear that high-temperature exposure led to partial elimination of oxygen and complete removal of hydrogen. In addition, the bulk composition of the exposed fiber was independent of firing time though it was dependent upon firing temperature. Chemical analysis suggests that the mass loss determined by TG is associated with the generation of H_2 , CO and SiO gases. In particular, the rapid mass loss at initial stage is attributable to the liberation of hydrogen. A shorter period of firing at lower temperature, consequently, caused greater loss of mass during high-temperature exposure.

3.2. Surface composition

Figs 3 and 4 show the AES depth profiles of the fibers fired at 1273 and 1573 K, respectively. The firing treatment at different temperatures showed marked difference in the AES depth profile. There was the oxide layer for the fiber fired at 1273 K. Then, the C/Si ratio was held nearly constant at 20 nm and deeper. The oxide layer, which was primarily formed in EB-cured PCS fiber, was eliminated by firing at 1573 K, as a result of generation of SiO and CO. The firing treatment at 1573 K produced a carbon-rich layer near the fiber surface. Particularly, after 3.6 ks of firing, the carbon layer of 20 nm was observed, and C/Si ratio was continuously changed to the constant value of about 1.4. The C/Si ra-

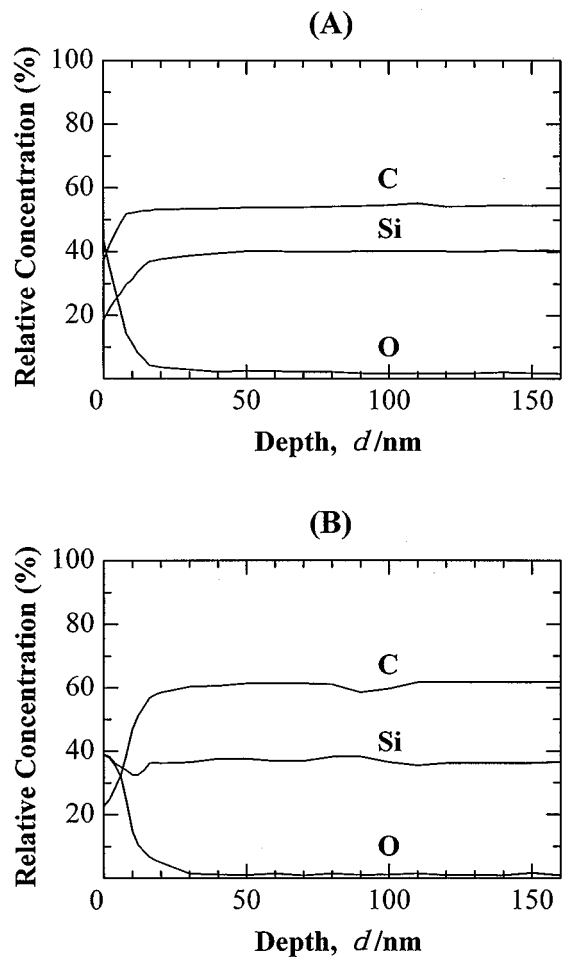


Figure 3 AES depth profiles of fibers fired at 1273 K. (A): 3.6 ks of firing (fiber A), (B): 36 ks of firing (fiber B).

tios at the surface of fibers fired for 3.6 ks at 1273 and 1573 K were lower than the bulk composition determined by chemical analysis (Table I). Prolonging the firing time to 36 ks resulted in an increase of C/Si ratio at fiber surface and its proximity to bulk composition.

Fig. 5 shows the composition depth profiles of SiC fibers which were fired at 1273 K and were subsequently exposed to 1873 K. By comparing Fig. 5A with Fig. 3A, it can be seen that an oxide layer became thin and C/Si ratio decreased to a depth of about 50 nm for the fiber fired for 3.6 ks. A large quantity of hydrogen retained in the as-fired SiC fiber (Table I). When exposed to 1873 K, H_2 gas is generated with great facility by the breakage of C-H bond [17, 18]. Consequently, a part of debonded carbon from C-H bond interacts with oxide layer to be liberated as CO gas, resulting in the reduction of C/Si ratio. On the other hand, for the fiber fired for 36 ks, the oxide layer was completely eliminated and alternatively a carbon-rich layer was produced just below the outer surface (Fig. 5B). This implies that the high-temperature exposure caused silicon removal as SiO gas from fiber surface. Fig. 6 shows the AES depth profiles of the fibers which were exposed to 1873 K after firing at 1573 K. By comparing Fig. 4 with Fig. 6, it can be seen that the carbon-rich layer in the fiber fired for 3.6 ks was thinned from 80 to 10 nm by the exposure at 1873 K and the C/Si ratio at the fiber surface approached the bulk composition determined

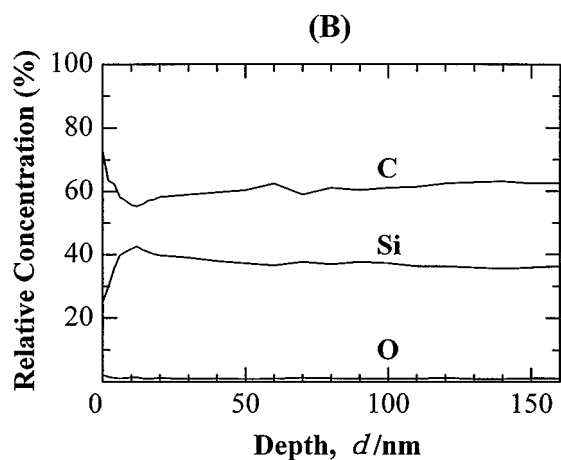
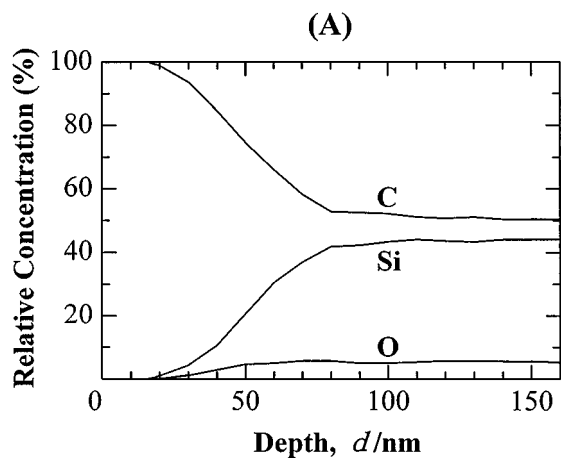


Figure 4 AES depth profiles of fibers fired at 1573 K. (A): 3.6 ks of firing (fiber C), (B): 36 ks of firing (fiber D).

by chemical analysis. This corresponds to a significant decrease in oxygen content (Table I, II), suggesting the generation of CO gases during exposure to 1873 K. On the other hand, in the fiber fired for 36 ks, there was little difference in the AES depth profile before and after the exposure to 1873 K. Comparing AES depth profile with chemical analysis shows that the change in composition was restricted to very thin layer of fiber surface. This is because a long period of firing decreased the oxygen content in fiber to a considerable extent. (Table I, II).

3.3. Crystallite size of β -SiC

Using Scherrer's formula, the apparent crystallite size, D_{111} , was estimated from the half-value width of (111) peak of β -SiC. The calculated values of the crystallite size are given in Fig. 7. The crystallite size in the as-fired state increased gradually with increasing the temperature and the duration of firing treatment, depending on the degree of ceramization. On the other hand, for the fiber exposed to 1873 K, the quite opposite tendency was observed with the relationship among crystallite size, firing temperature and time. This result agrees with the fact that the crystallization into β -SiC is faster in Si-C-O fiber fired at 1273 K (Nicalon NL400) than in one fired at 1573 K (Nicalon NL200) [21]. At elevated temperature, the fiber in imperfectly fired state is

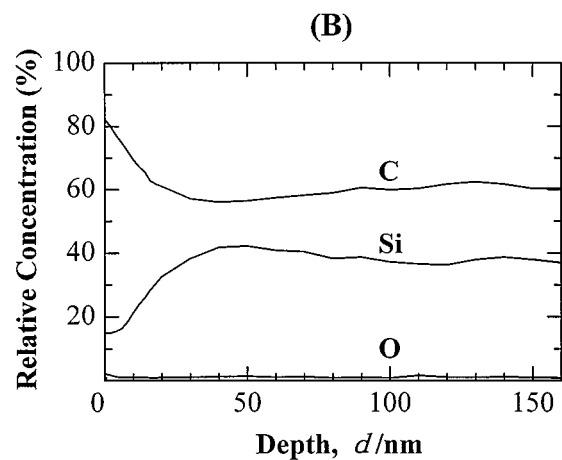
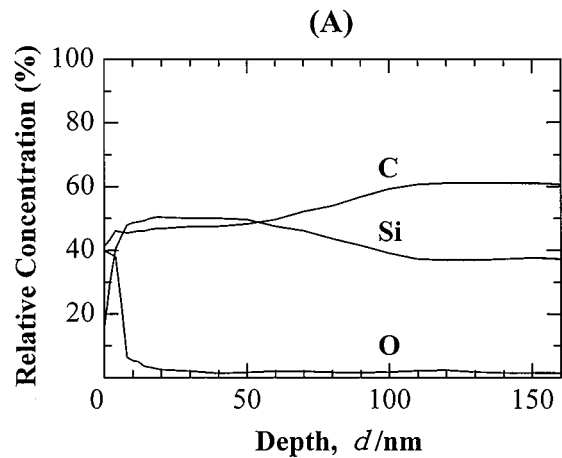


Figure 5 AES depth profiles of fibers exposed of 3.6 ks at 1873 K. (A): 3.6 ks of firing at 1273 K (fiber A), (B): 36 ks of firing at 1273 K (fiber B).

unstable because of large departure from equilibrium state, resulting in rapid crystallization into β -SiC (i.e., decomposition).

3.4. Specific resistivity

The specific resistivity, ρ , is the property which is very sensitive to the microstructural change of SiC fiber. Fig. 8 shows the relationship among the specific resistivity, firing temperature and firing time. When fired for 3.6 ks, ρ of the fiber fired at the lowest temperature of 1273 K was 2 orders of magnitude higher than ρ of other fibers, reflecting imperfect ceramization as a result of large amounts of residual hydrogen (Table I). For firing treatment at 1273 and 1373 K, ρ was the high level of about $1 \Omega \text{ m}$ even after 36 ks. Firing at 1473 and 1573 K lowered ρ to the value of $10^{-2} \Omega \text{ m}$ which was nearly close to the level in fibers exposed to 1873 K. The resistivity of the fiber exposed to 1873 K was practically independent of the temperature and time of firing, and ranged from 10^{-3} to $10^{-2} \Omega \text{ m}$.

3.5. Surface morphology

Fig. 9 shows SEM photographs of the fibers exposed to 1873 K. All fibers had a microstructure mixed with huge particles and fine grains. It is evident from photos

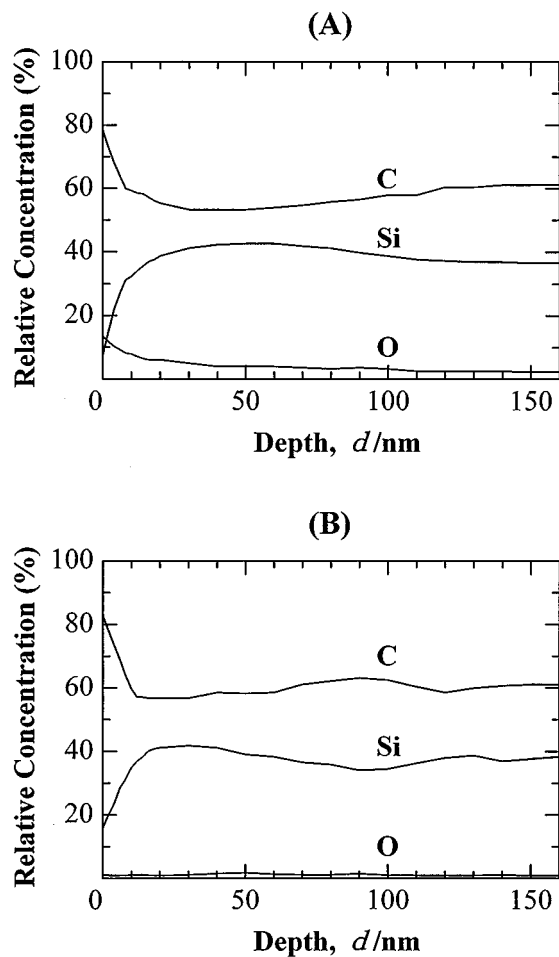


Figure 6 AES depth profiles of fibers exposed for 3.6 ks at 1873 K. (A): 3.6 ks of firing at 1573 K (fiber C), (B): 36 ks of firing at 1573 K (fiber D).

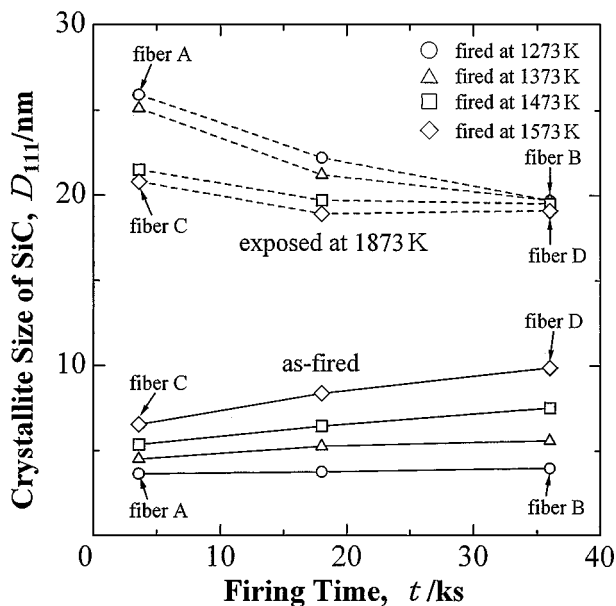


Figure 7 Crystallite size of SiC in as-fired fibers and fibers exposed for 3.6 ks at 1873 K.

(B) and (E) that the huge particles grew outwards at fiber surface and the fine grains were present in the core, too. As discussed later, the huge particles and fine grains were produced by the gas-phase reaction and

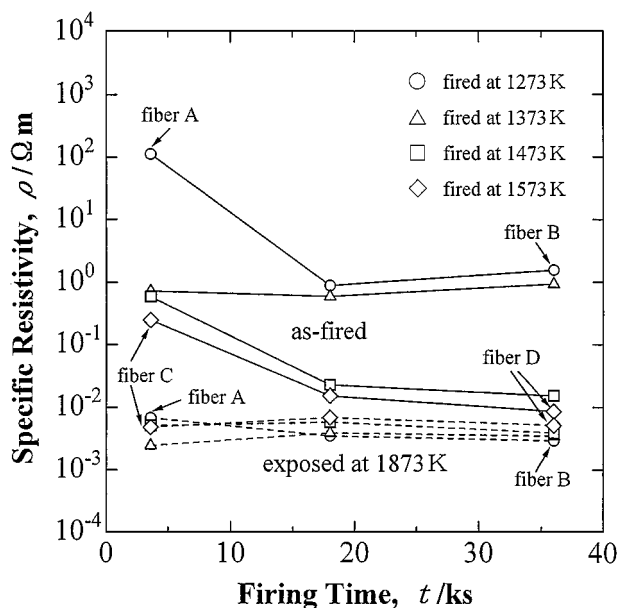


Figure 8 Specific resistivity of as-fired fibers and fibers exposed for 3.6 ks at 1873 K.

the pyrolysis reaction, respectively. The microstructure derived from the pyrolysis reaction were finer in 36 ks of firing than in 3.6 ks of firing, corresponding to the apparent crystallite size shown in Fig. 7.

3.6. Tensile strength

Fig. 10 shows the relationship between the tensile strength of as-fired fiber and firing time. A prolonged firing at 1273 and 1373 K produced an increase in strength. On the other hand, a long period of firing at 1473 K caused considerable degradation of strength. In addition, the firing treatment resulted in lower strength at 1573 K than at 1373 K.

The tensile strength of the fiber exposed to 1873 K is shown in Fig. 11. The strength of exposed fiber hardly depended on firing time, although it increased with rise in firing temperature below 1473 K. The firing at 1573 K was no longer effective in increasing the retained strength after exposure to 1873 K.

4. Discussion

Large amounts of hydrogen was retained in fiber fired at low temperature. In particular, 11.7% of hydrogen was retained for the firing of 3.6 ks at 1273 K. The cured PCS fiber evolved CH_4 gas in the temperature range of 800–1200 K with a peak at about 1000 K and evolved H_2 gas in the temperature range of 800–1700 K [17, 18]. CH_4 evolution was reflected in a large reduction of C/Si ratio before and after firing treatment (see Table I). While the evolution of CH_4 and H_2 at 800–1000 K is attributable to the decomposition of chemical bonds of Si atoms, i.e., Si– CH_3 and Si–H, the evolution of H_2 at 1000–1800 K was attributable to the decomposition of C–H bonds in Si– CH_2 –Si [18]. Therefore, while the evolution of CH_4 gas was completed during heating to firing temperatures from 1273 to 1573 K, H_2 gas only was continuously generated by the breakage of C–H

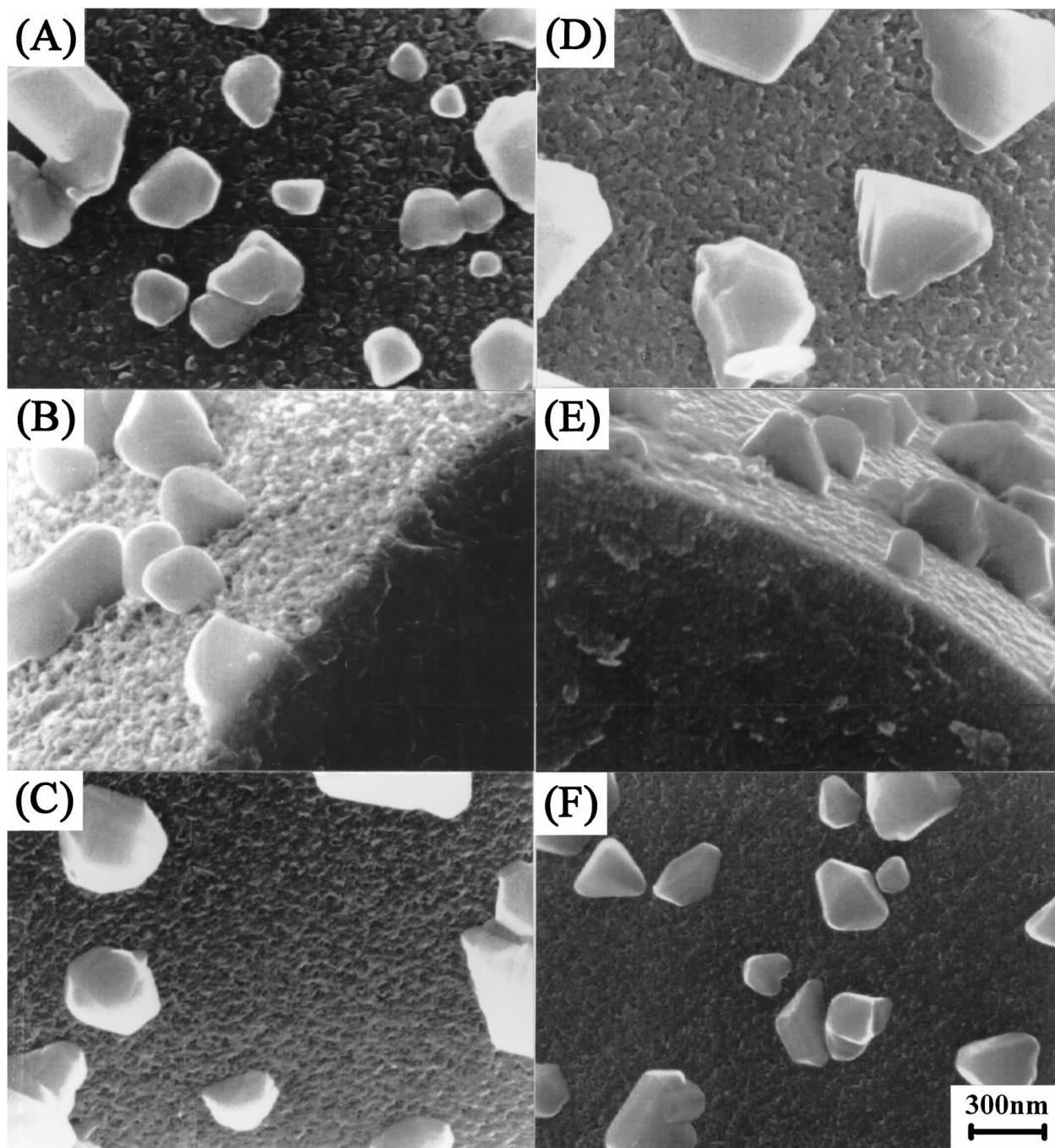


Figure 9 SEM photographs of fibers exposed for 3.6 ks at 1873 K. (A), (B): 3.6 ks of firing at 1273 K (fiber A), (C): 36 ks of firing at 1273 K (fiber B) (D), (E): 3.6 ks of firing at 1573 K (fiber C), (F): 36 ks of firing at 1573 K (fiber D) fibers are crystallized into β -SiC and huge β -SiC crystals are formed on fiber surface.

bonds during keeping at each firing temperature. As can be seen from Table I, consequently, the C/Si ratio of fiber fired for 3.6 ks at 1273 K was nearly identical to that fired for 36 ks at 1273 K. On the other hand, a long time firing at 1573 K decreased the C/Si ratio, probably owing to CO gas generation. Thus, prolonging the firing time, particularly at lower temperatures, enhanced the ceramization of PCS fiber, resulting in the crystal growth of β -SiC, a reduction of resistivity and a large increase in tensile strength. Then, AES depth profiles showed that different firing conditions changed largely the surface composition of both as-fired fiber and exposed fiber, reflecting the different amounts of H₂ gas evolved (Figs 3–6). Furthermore, the surface com-

position after a long period firing was nearly equal to the bulk composition except for very thin layer of fiber surface.

When the fiber is exposed to elevated temperature, the retained hydrogen is readily liberated. Thus, the hydrogen liberation caused the abrupt mass loss in the initial stage of TG curves (Fig. 2). In addition, the shorter period firing at lower temperature caused more largely mass loss. The amorphous SiC_xO_y phase has a tendency to crystallize into β -SiC which is thermodynamically stable at high temperatures. Silicon and carbon atoms in SiC_xO_y phase diffuse to β -SiC crystallite and the crystal growth can take place. Consequently, the remained oxygen is concentrated in oxycarbide phase

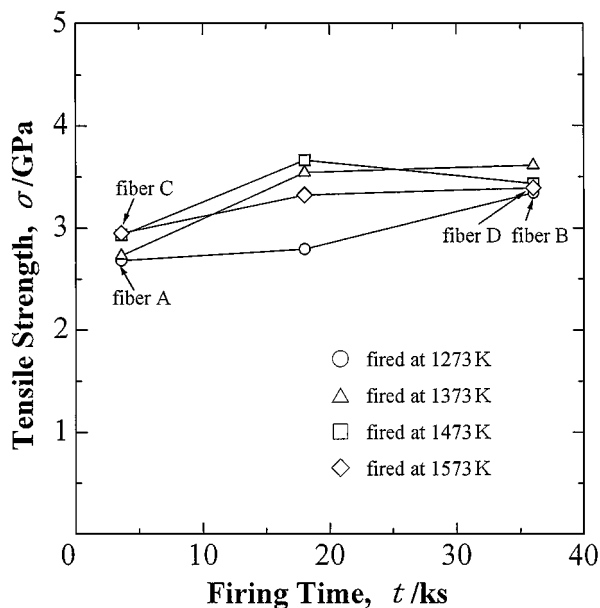


Figure 10 Tensile strength of as-fired fibers.

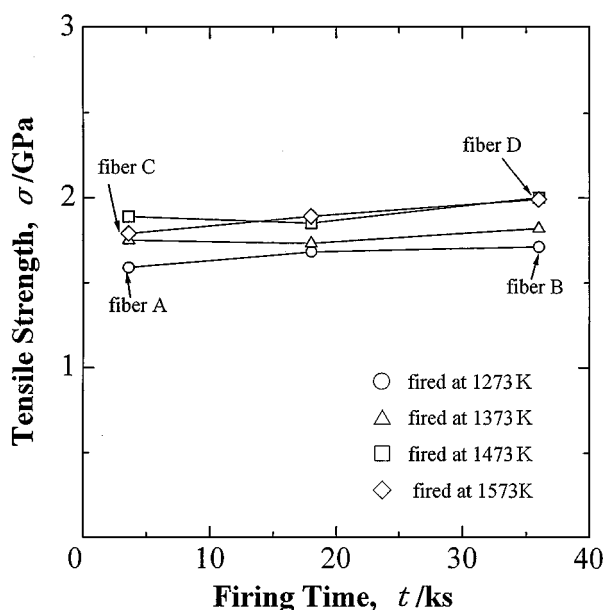
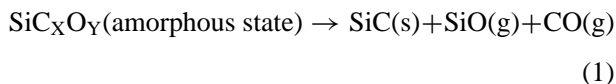


Figure 11 Tensile strength of fibers exposed for 3.6 ks at 1873 K.

until it is liberated as SiO and CO gases. Thus, the pyrolysis reaction proceeds:



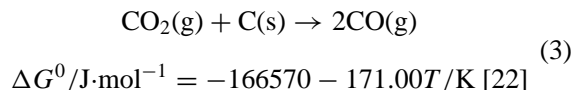
It is evident from Table II that SiC fiber retained a slight amount of SiC_xO_y phase even after exposure at 1873 K. However, the exposed fiber was practically the mixture of SiC and free carbon because of low oxygen concentration. The presence of a large amount of free carbon made the specific resistivity low to $10^{-3} \Omega\text{m}$ (Fig. 8). Long time of firing at high temperature approached the resistivity of as-fired fiber to that of the fiber exposed to 1873 K. Thus, the microstructure of this as-fired fiber also appears to be nearly the mixture of free carbon and SiC. Furthermore, prolonged firing at 1573 K decreased oxygen content and C/Si ra-

tio of fiber (Table I). This suggests that SiC_xO_y phase decomposed to generate chiefly CO gas. The decomposition produced a considerable decrease in tensile strength of as-fired fiber (Fig. 10).

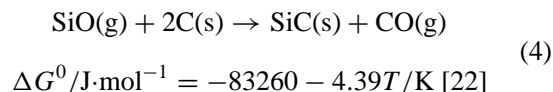
The outward growth of huge particle was observed at fiber surface (Fig. 9). The huge particle seems to be β -SiC produced by the reactions between pyrolysis gas, SiO and CO:



The use of a graphite crucible causes the reproduction of CO_2 to CO gas:



Combining reactions (2) and (3) yields the following reaction:



Reaction (4) also occurs between SiO gas and carbon at fiber surface. Since the thermodynamical calculation of reaction (4) gives $p_{\text{CO}_2}/p_{\text{CO}} = 1.94 \times 10^4$ at 1873 K, p_{CO_2} is negligibly small. Therefore, the equilibrium SiO pressures of reaction (4) are calculated to be 8.01×10^{-3} atm at $p_{\text{SiO}} + p_{\text{CO}} = 1$ atm ($p_{\text{Ar}} = 0$ atm), 8.01×10^{-4} atm at $p_{\text{SiO}} + p_{\text{CO}} = 0.1$ atm ($p_{\text{Ar}} = 0.9$ atm) and 8.01×10^{-5} atm at $p_{\text{SiO}} + p_{\text{CO}} = 0.01$ atm ($p_{\text{Ar}} = 0.99$ atm), respectively. The above reactions is thought to proceed, owing to low equilibrium pressure of SiO. Compared to pyrolytic SiC, the huge SiC crystal was produced in a slight quantity. Therefore, its effect on the properties of fiber is almost negligible.

The strength degradation of PCS-derived SiC fiber at elevated temperature resulted from the coarsening of β -SiC crystals and the damaging effect of the gas generation to the fiber structure. The tensile strength, σ , of SiC fiber fabricated by EB-curing method was nearly proportional to the crystallite size of β -SiC, D_{111} [16, 20]. That is to say, the following empirical expression was given:

$$\sigma = a + b \cdot D_{111}^{-1/2} \quad (5)$$

Fig. 12 shows the relationship between tensile strength and SiC crystallite size. The strength of as-fired fiber scattered largely. In particular, despite the small crystallite size, the fibers fired at lower temperatures had the low levels of strength. The fiber exposed to 1873 K indicates that its strength was roughly proportional to the reciprocal of square root of SiC crystal size in a narrow range of tensile strength, i.e., 1.6–2.0 GPa.

The amount of gas evolved was evaluated by using the mass loss determined during 3.6 ks of exposure at 1873 K. Fig. 13 shows the relationship between tensile strength and mass loss, $100 \cdot \Delta W/W_0$. Marked degradation of strength to about 60% of as-fired strength

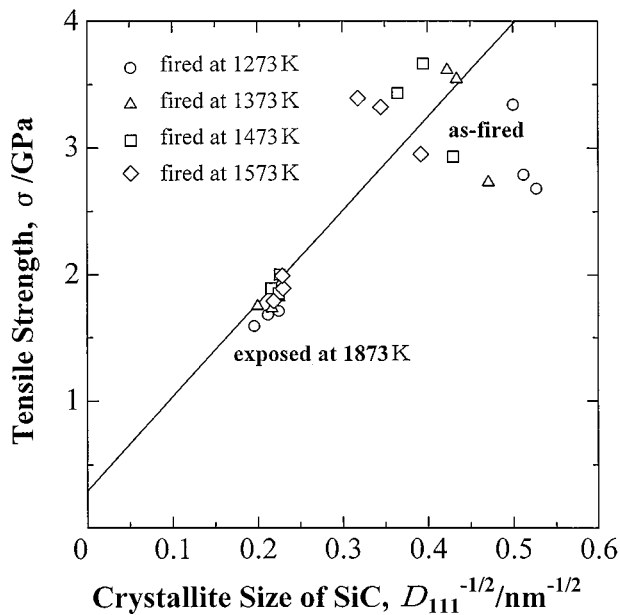


Figure 12 Relationship between tensile strength and SiC crystallite size of as-fired fibers and fibers exposed for 3.6 ks at 1873 K.

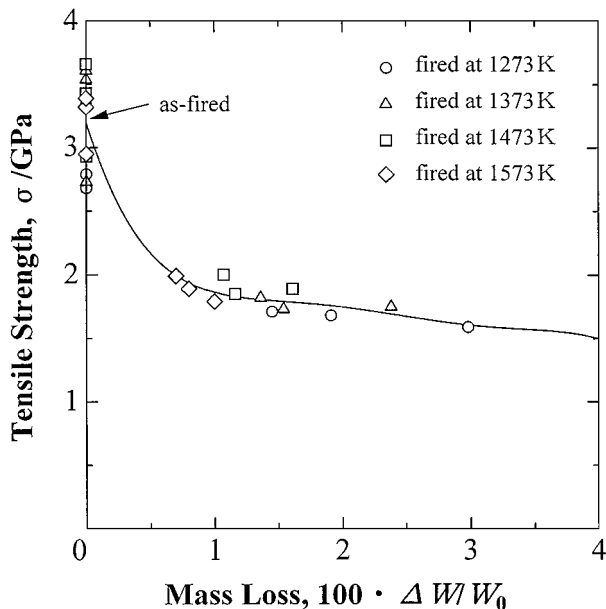


Figure 13 Relationship between tensile strength and amount of gas evolved during firing treatment and 3.6 ks of exposure to 1873 K.

was observed after the exposure to 1873 K. In addition, the fiber strength was only slightly lowered as the amount of gas evolved increased. This degradation of fiber strength seems to be due to the abrupt gas evolution in the early stage at high-temperature exposure, i.e., principally hydrogen generation (see Fig. 2).

From the above consideration, prolonging firing at low temperature was found to be effective for improvement of fiber strength in the as-fired state and after high-temperature exposure. On the other hand, in the fibers fired at 1573 K, although a little amount of gas was evolved (Fig. 2) and the SiC crystallite size was small (Fig. 7), the improvement of fiber strength was not observed both in the as-fired state and after exposure to 1873 K (Fig. 10, 11). During firing treatment at

1573 K, the decomposition of SiC_xO_y phase (i.e., pyrolysis reaction) occurred. Consequently, this pyrolysis appears to cause the reduction in the strength of fibers fired over a long period of time. A long period firing at 1573 K, therefore, should be avoided.

5. Summary

In order to fabricate excellent low-oxygen SiC fibers from EB-cured PCS fibers, the effect of firing conditions on the characteristics of SiC fibers in the as-fired state and after exposure to 1873 K has been investigated. The following results were obtained:

(1) While the amount of gas evolved during firing increased with increasing temperature and time of firing, that of gas evolved during subsequent exposure at 1873 K was reduced. This is because the firing at lower temperature retained larger amounts of hydrogen. Slow generation of SiO and CO followed abrupt dehydrogenation at early stage of high-temperature exposure.

(2) The high-temperature firing produced a carbon-rich layer at fiber surface. The surface composition was nearly identical to the bulk composition after exposure to high-temperature.

(3) In contrast to the SiC crystallite size of as-fired fiber, that of high-temperature exposed fiber decreased in size by increasing temperature and time of firing.

(4) Imperfect ceramization resulted in high level of specific resistivity for low-temperature fired fiber. The resistivity after prolonged firing at high temperature was nearly equal to that after exposure at 1873 K.

(5) A long period firing below 1473 K was effective in strengthening as-fired and high-temperature exposed fibers. Prolonged firing at 1573 K, however, caused the reduction in as-fired strength.

References

1. T. MAH, N. L. HECHT, D. E. McCULLUM, J. R. HEONIGMAN, H. M. KIM, A. P. KATZ and H. A. LIPSITT, *J. Mater. Sci.* **19** (1984) 1191–201.
2. K. L. LUTHRA, *J. Amer. Ceram. Soc.* **69** (1986) C.231–C.233.
3. S. M. JOHNSON, R. D. BRITAIN, R. H. LAMOREAUX and D. J. ROWCLIFF, *ibid.* **71** (1988) C.132–C.135.
4. D. J. PYSHER, K. C. GORETTA, R. S. HODDER and R. E. TRESSLER, *ibid.* **72** (1989) 284–88.
5. C. LAFFON, A. M. FLANK, P. LAGARDE, M. LARIDJANI, R. HAGEGE, P. OLRÉ, J. KOTTERET, J. DIXMIER, J. L. MIQUEL, H. HOMMEL and A. P. LEGRAND, *J. Mater. Sci.* **24** (1989) 1503–1512.
6. M. MONTHIOUX, A. OBERLIN and E. BOUILLON, *Compos. Sci. Technol.* **37** (1990) 21–35.
7. T. SHIMOO, M. SUGIMOTO and K. OKAMURA, *Nippon Kinzokugakkai-shi* **54** (1990) 802–808.
8. *Idem.*, *Seramikkusu-ronbun-shi* **98** (1990) 1324–1329.
9. B. A. BENDER, J. S. WALLECE and D. J. SCHRODT, *J. Mater. Sci.* **26** (1991) 970–976.
10. E. BOUILLON, F. LANGLAIS, R. PAILLER, R. NASLAIN, F. CRUEGE, P. V. HUONG, J. C. SARTHOU, A. DELPUECH, C. LAFFON, P. LAGARDE, M. MONTHIOUX and A. OBERLIN, *ibid.* **26** (1991) 1333–1345.
11. T. SHIMOO, H. CHEN and K. OKAMURA, *J. Ceram. Soc. Jpn* **100** (1992) 48–53.
12. C. VAHLAS, P. ROCABOIS and C. BERNARD, *J. Mater. Sci.* **29** (1994) 5839–5846.

13. M. TAKEDA, Y. IMAI, H. ICHIKAWA, T. SEGUCHI and K. OKAMURA, *Ceram. Eng. Sci. Proc.* **12** (1991) 1007–1012.
14. *Idem.*, *ibid.* **13** (1992) 209–217.
15. T. SHIMOO, T. HAYATSU, M. NARISAWA, M. TAKEDA, H. ICHIKAWA, T. SEGUCHI and K. OKAMURA, *J. Ceram. Soc. Jpn* **101** (1993) 1379–1383.
16. G. CHOLLON, R. PAILLER, R. NASLAIN, F. LAANAMI, M. MONTHIOUX and P. OLRÉY, *J. Mater. Sci.* **32** (1997) 327–347.
17. M. SUGIMOTO, T. SHIMOO, K. OKAMURA and T. SEGUCHI, *J. Amer. Ceram. Soc.* **78** (1995) 1013–1017.
18. *Idem.*, *ibid.* **78** (1995) 1849–1852.
19. G. CHOLLON, M. CZERNIAK, R. PAILLER, X. BOURRAT, R. NASLAIN, J. P. PILLOT and R. CANNET, *J. Mater. Sci.* **32** (1997) 893–911.
20. T. SHIMOO, I. TSUKADA, M. NARISAWA, T. SEUCHI and K. OKAMURA, *J. Ceram. Soc. Jpn* **104** (1997) 1070–1074.
21. T. SHIMOO, M. SUGIMOTO and K. OKAMURA, *Nippon Seramikusu-Kyokai-shi* **98** (1990) 1324–1329.
22. E. T. TURKDOGAN, “Physical Chemistry of High Temperature Technology” (Academic Press, New York, 1980) pp. 5–24.

*Received 17 September 1997
and accepted 16 April 1999*